Environmental Pollution 208 (2016) 840–849

Contents lists available at ScienceDirect

Environmental Pollution

journal homepage: www.elsevier.com/locate/envpol

Physiological differences in response to di-*n*-butyl phthalate (DBP) exposure between low- and high-DBP accumulating cultivars of Chinese flowering cabbage (*Brassica parachinensis* L.)

Hai-Ming Zhao [a], Huan Du [a], Lei Xiang [a], Yan-Wen Li [a], Hui Li [a], Quan-Ying Cai [a, **], Ce-Hui Mo [a, *], Gang Cao [a], Ming-Hung Wong [a, b]

[a] Guangdong Provincial Research Center for Environment Pollution Control and Remediation Materials, Guangzhou Key Laboratory of Environmental Exposure and Healthy, School of Environment, Jinan University, Guangzhou 510632, China
[b] Consortium on Health, Environment, Education and Research (CHEER), and Department of Science and Environmental Studies, Hong Kong Institute of Education, Hong Kong, China

ARTICLE INFO

Article history:
Received 13 August 2015
Received in revised form
4 November 2015
Accepted 5 November 2015
Available online 20 November 2015

Keywords:
Chinese flowering cabbage (*Brassica parachinensis* L.)
Di-*n*-butyl phthalate
Genotypic variation
Cell ultrastructure
Physiological response

ABSTRACT

To increase understanding on the mechanisms of cultivar difference in contaminant accumulation in crops, this study was designed to compare the physiological responses to di-*n*-butyl phthalate (DBP) exposure between low (*Lvbao70*) and high (*Huaguan*) DBP cultivars of Chinese flowering cabbage (*Brassica parachinensis* L.). Under high DBP exposure, significant differences in various physiological responses were observed between the two cultivars, which might account for the variation in DBP accumulation. Ultrastructure observation also showed different alterations or damages in the mesophyll cell structures between both cultivars, especially for the chloroplast disintegration, starch grain quantity, and plastoglobuli accumulation. Compared with *Huaguan*, *Lvbao70* suffered greater decreases in biomass, chlorophyll content, carbon assimilation, gas exchange parameters, photosynthetic electron transport capacity, and antioxidase activities, which would have resulted in a great reduction of photosynthetic capacity. Although *Lvbao70* enhanced energy dissipation and activities of some antioxidant enzymes, they did not provide sufficient protection against oxidative damage caused by DBP. The result suggested that the lower DBP tolerance of *Lvbao70* might be associated with its poor physiological performances, which was responsible for its lower DBP accumulation to protect itself from toxicity. Additionally, *Lvbao70* had a significantly lower transpiration rate and stomatal conductance than *Huaguan*, which might be the factors regulating DBP-accumulation variation.

1. Introduction

Phthalic acid esters (PAEs) are commonly used as plasticizer. In recent years, PAE levels in agricultural soils have increased significantly due to the application of agricultural plastic films (Wang et al., 2013; Niu et al., 2014). Some PAE compounds and their degradation intermediates are suspected to cause cancer and disrupt the endocrine system (Niu et al., 2014; Mo et al., 2009). Di-*n*-butyl phthalate (DBP), a representative PAE compound, has become one of the dominant PAEs in agricultural soil (Wang et al., 2013; Niu et al., 2014; Cai et al., 2008). For the general population, diet is a primary route of exposure to PAEs (Schecter et al., 2013). DBP can be accumulated in vegetables, which poses a potential threat to food safety and human health (Mo et al., 2009).

To reduce the risk of soil contaminants entering human food chain, selection of crop cultivars with low contaminant accumulation in their edible parts has been proposed as a practical solution (Wang et al., 2009). Chinese flowering cabbage (*Brassica parachinensis* L.) is a main vegetable in southern China, which is also exported to many countries and regions, and it tends to accumulate DBP in PAE-contaminated soils (Mo et al., 2009). Thus, screening low-DBP cultivars and understanding their formation mechanism are very important for food safety. In our previous study, some typical low and high DBP-accumulating cultivars of Chinese flowering cabbages (*B. parachinensis* L.) were screened out (Zhao et al.,

* Corresponding author.
** Corresponding author.
E-mail addresses: yingqy@126.com (Q.-Y. Cai), tchmo@jnu.edu.cn (C.-H. Mo).

http://dx.doi.org/10.1016/j.envpol.2015.11.009
0269-7491/

2015). However, the mechanisms of cultivar differences in DBP accumulation remain unclear.

The physiological processes are the intrinsic factors regulating the uptake and accumulation of contaminants by plants (Mostofa et al., 2015; Pietrini et al., 2015). The previous studies mostly focused on the toxic effects of DBP on crop physiological processes including seed germination and growth (Liu et al., 2014; Ma et al., 2013), ultrastructure of mesophyll cells (Zhang et al., 2015a), root physiology (Zhang et al., 2015b), fruit quality (Yin et al., 2003), antioxidant activity (Ma et al., 2013, 2014; Liu et al., 2014; Zhang et al., 2015a), and protein profile (Liao et al., 2009), while very limited data are available on the effects of plant photosynthesis to DBP exposure. And, cultivar variation in physiological responses to DBP exposure was also hardly studied. It was reported that other organic contaminants could decrease photosynthesis rates and alter the photosynthetic apparatus (Ahammed et al., 2012; Li et al., 2013). Thus, the photosynthetic responses can be used as indicators to evaluate plant tolerance to pollutants (Pietrini et al., 2015). Especially, the use of chlorophyll fluorescence analysis, in combination with simultaneous gas exchange measurements, allows the evaluation of the heterogeneity in the photosynthetic function of photosystem II (PSII) in plants subjected to environmental stress (Strasser et al., 2000; Jiang et al., 2008; Tomar and Jajoo, 2013).

Furthermore, to protect against oxidative stress induced by DBP, plant cells are equipped with intrinsic antioxidant capacity that comprises a variety of antioxidant enzymes, which can provide useful evidence to evaluate the tolerance of plants to DBP toxicity (Gill and Tuteja, 2010; Ma et al., 2014). In particular, catalase (CAT) and superoxide dismutase (SOD) are the most valuable antioxidases in the protective system of higher plants to survive oxidative stress, and their changes can affect the resistance and adaptation of plants to DBP stress (Ma et al., 2013; Zhang et al., 2015a); glutathione S-transferase (GST) is well known in detoxification reaction in plant (Kumar et al., 2013); malondialdehyde (MDA) formation characterizes the oxidative stress caused by lipid peroxidation (Ma et al., 2013). Besides, observation on cell ultrastructure can reflect directly the toxicity of DBP to plant. Although there are so many physiological responses to DBP stress, it is not clear whether DBP-induced alterations in these physiological processes are associated with DBP accumulation in plant.

In this study, greenhouse pot experiments were conducted to investigate various physiological differences (including biomass, cell ultrastructure, gas exchange, photosynthesis, and antioxidant enzyme activities) between the low- and high-DBP cultivars of Chinese flowering cabbage grown in DBP-contaminated soil. We hypothesize that there were significant differences in the physiological responses to DBP between the low and high accumulators, which were responsible for the variation in DBP accumulation.

2. Materials and methods

2.1. Chemicals and materials

DBP (98.7%) was obtained from Aladdin Chemistry Co., Ltd., China, while DBP stock standard solution (1000 μg/mL in dichloromethane, 99.8%) for analysis was purchased from Sigma Chemical Co., USA. Other chemicals were obtained from Tianjin Chemical Reagent Co., China. The low- and high-DBP cultivars of Chinese flowering cabbages (*B. parachinensis* L), *Lvbao70* and *Huaguan*, respectively, were selected for this study (Zhao et al., 2015).

2.2. Experimental design

The soil for pot experiments collected from an agricultural field of South China Agricultural University (Guangzhou, China) was air-dried and ground to pass through a sieve (5 mm). The soil contained 15.7 g kg^{-1} (dry weight, DW) of organic matter, 8.22 cmol kg^{-1} of cation exchange capacity, 1.45 g kg^{-1} of total N, 2.01 g kg^{-1} of total P, and 18.87 g kg^{-1} of total K. The background concentration of DBP in this soil was 0.19 mg kg^{-1}. The pot experiment was performed in a greenhouse with natural light.

According to our previous investigation, the mean value of DBP in vegetable soils in southern China was 9.5 mg kg^{-1} (Cai et al., 2008). Thus the soil spiked at 10 mg kg^{-1} was designated as low-DBP treatment. Additionally, to evaluate the differential responses of the two cultivars to higher level of DBP stress, the soil spiked at 100 mg kg^{-1} was used as high-DBP treatment. An aliquot of soil (passed through a 2-mm sieve, 10% total quantity of soil) was spiked with a solution of DBP in acetone. After acetone evaporated, the spiked soils were mixed thoroughly with uncontaminated soils, sieved again to homogenize the soils, and aged for two weeks under dark condition. The soil without DBP spiked was used as a control. A total of 3.0 kg (DW) of the above soil was put into a ceramic pot (20 cm in diameter, and 14 cm in height) and mixed with 6.0 g of compound fertilizer (N:P:K = 4:3:4). Next, 20 seeds of each cultivar were sown into the soil of each pot. All treatments were in three replicates. Pots were randomly arranged in a glasshouse at natural temperatures (25–32 °C), and the soils were watered daily with deionized water to maintain moderate moisture. After germination, seedlings were gradually thinned with five seedlings remained (day 15) in each pot. At the end of experiment (day 45), six to eight leaves of each pot were used for measuring pigments, gas exchange, OJIP transients, antioxidant enzyme activities, and methane dicarboxylic aldehyde (MDA) content. Finally, plant samples were washed with deionized water and then divided into roots and shoots, and fresh weights were recorded.

2.3. Analysis of DBP

The procedures of ultrasonic-assisted sample extraction using silicagel column and DBP analysis using gas chromatography coupled with mass spectrometry (GC/MS, Shimadzu QP2010 Plus, Japan) were conducted following the method adopted in our previous study (Cai et al., 2007) with minor modifications (see Supplementary M1). The detection limit of DBP was 1.2 μg kg^{-1}. The average concentration of DBP was 3.2 (ranged from 1.27 to 7.80) μg kg^{-1} in all procedural blanks (n = 12), which was subtracted from sample values. The recoveries of DBP in plant samples ranged from 87.4% to 107.2%.

2.4. Chlorophyll content

Leaf chlorophyll content was measured following the method described by Hu et al. (2014), with minor modifications (see Supplementary M1).

2.5. Transmission electron microscope (TEM)

Ultrastructural studies were performed on leaf tissues of the two cultivars by TEM following the protocol of Zhang et al. (2015a). Briefly, the samples with different DBP treatments were collected and cut to 1 mm^3 cubes, fixed in 4% (v/v) glutaraldehyde and then 1% (v/v) osmium tetroxide, and dehydrated successively in ethanol series (30%–100%, v/v) and embedded in Epon-812 Resin. After making ultrathin sections (50–70 nm) with a Leica UCT ultramicrotome, the sections were mounted on copper grids and stained with 4% (w/v) uranyl acetate and lead citrate, and then examined at 100 kV using a FEI-Tecnai G2 12-type TEM (Eindhoven, Netherlands).

2.6. Measurement of gas exchange

The gas exchange system (LI-6400XT; Li-Cor Inc., USA) was used to determine net photosynthetic rate (Pn), transpiration rate (E), stomatal conductance (Gs), and intercellular CO_2 concentration (Ci) following the method described by Li et al. (2013). The third or fourth leaf of each treatment was measured for 11 times. LI-6400XT (6400-02B) was used to control chamber conditions. Light intensity, leaf temperature, and CO_2 concentration inside the leaf chamber were 1000 μmol m^{-2} s^{-1}, 30 °C, and 380 μmol mol^{-1}, respectively.

2.7. Leaf chlorophyll a fluorescence transient

Chlorophyll a fluorescence parameters were estimated immediately after the gas exchange measurements using a Handy Plant Efficiency Analyser (Hansatech, U.K.) according to Tomar and Jajoo (2013). The leaves (also used for gas exchange measurements) were first dark-adapted for 20 min and then measured for 11 times. The fluorescence signal was received by the sensor head during recording and was digitized in the control unit using a fast digital converter. The control leaves exhibited a polyphasic rise known as OJIP Chl a fluorescence transient: O to J phase (ended at 2 ms), J to I phase (ended at 30 ms), and I to P phase (ended at 500 ms). The JIP test was named after the basic steps in the fluorescence transient when plotted on a logarithmic time scale (Tomar and Jajoo, 2013). The OJIP transient was induced by red light of about 3000 μmol m^{-2} s^{-1} provided by an array of three light-emitting diodes (peak 650 nm), which focused on the leaf surface to give homogenous illumination over the exposed area of the leaf. From the OJIP transient, the extracted parameters (F_o, F_m, $F_{50\mu s}$, $F_{100\mu s}$, $F_{300\mu s}$, F_J, F_I, t_{Fm}, etc.) led to the calculation and derivation of a range of new parameters, according to previous studies (Jiang et al., 2008; Tsimilli-Michael and Strasser, 2008) (Table 1).

2.8. Activities of antioxidant enzymes and MDA content

Plant samples were extracted according to the method of Ma et al. (2014) with minor modifications. The activities of antioxidant enzymes (including SOD, CAT, and GST) and MDA content were measured with a spectrophotometer (Shimadzu UV-2450, Japan) according to the manufacturer's instructions of the corresponding kits (Nanjing Jiancheng Bioengineering Institute, China) (see Supplementary M1).

2.9. Statistical analysis

Results are expressed as means ± standard error (SE). One-way analysis of variance (ANOVA) followed by Duncan's test was performed with Microsoft Excel 2003 and SPSS 17.0.

3. Results

3.1. Plant biomass and DBP concentration

DBP concentrations in shoots and roots of both cultivars increased with an increase in the concentration of DBP spiked in soil (Fig. S1A). Similar as our previous study (Zhao et al., 2015), *Lvbao70* had lower DBP concentrations in shoots but higher in roots than those of *Huaguan* under the same DBP treatment (Fig. S1A). Thus, *Lvbao70* should be a desirable choice in terms of food safety. Compared with the control, low-DBP exposure promoted the growth of *Lvbao70* with a significant increase in shoot biomass ($P < 0.05$), but no significant effects were observed on shoot and root biomass of *Huaguan* (Fig. S1B). However, the shoot and root biomass of the two cultivars decreased significantly in high DBP treatment ($P < 0.05$). Especially, the shoot biomass of *Lvbao70* was significantly lower ($P < 0.05$) than that of *Huaguan*. On the other hand, the opposite correlations were observed in low DBP

Table 1
Parameters and formulae used in the analysis of OJIP fluorescence induction dynamics curves.

Formulate and terms	Illustration
Measured values	
F_0	Minimal recorded fluorescence intensity
F_m	Maximal recorded fluorescence intensity
$F_{50\mu s}$, $F_{100\mu s}$ and $F_{300\mu s}$	Fluorescence intensities at 50, 100 and 300 μs, respectively
F_J and F_I	Fluorescence intensities at the J-step (2 ms) and at the I-step (30 ms), respectively
t_{Fm}	Time to reach maximal fluorescence intensity *F*m
Area	Area above the fluorescence curve to *F*m
Technical fluorescence parameters	
$V_J = (F_J - F_0)/(F_m - F_0)$	Relative variable fluorescence intensity at the J-step
$M_0 = 4(F_{300\mu s} - F_0)/(F_m - F_0)$	Approximated initial slope of the fluorescence transient
$S_m = (Area)/(F_m - F_0)$	Normalized area above the OJIP transient (reflecting multiple-turnover Q_A reduction events) or total electron carriers per reaction center (RC)
Energy absorption parameters	
$ABS/RC = M_0 \cdot (1/V_J) \cdot (1/\varphi_{P0})$	Absorption flux per RC
$TR_0/RC = M_0 \cdot (1/V_J)$	Trapped energy flux per RC (at $t = 0$)
$ABS/CS_0 \approx F_0$	Absorption flux per cross section (CS) (at $t = 0$)
$TR_0/CS_0 = \varphi_{P0} \cdot (ABS/CS_0)$	Trapped energy flux per CS (at $t = 0$)
Energy transformation parameters	
$RC/CS_0 = \varphi_{P0} \cdot (V_J/M_0) \cdot (ABS/CS_0)$	Density of active PSII RCs per CS (at $t = 0$)
$\varphi_{P0} = TR_0/ABS = 1 - F_0/F_m = F_v/F_m$	Maximum quantum yield for primary photochemistry (at $t = 0$)
$\varphi_{E0} = ET_0/ABS = (F_v/F_m)\,(1 - V_J)$	Quantum yield for electron transport (at $t = 0$)
$ET_0/RC = M_0 \cdot (1/V_J) \cdot \psi_0$	Electron transport flux per RC (at $t = 0$)
$ET_0/CS_0 = (ABS/CS_0)\,\varphi_{E0}$	Electron transport flux per CS (at $t = 0$)
$\psi_0 = ET_0/TR_0 = (1 - V_J)$	Probability that a trapped exciton moves an electron into the electron transport chain beyond QA^- (at $t = 0$)
Energy dissipation parameters	
$DI_0/RC = (ABS/RC) - (TR_0/RC)$	Dissipated energy flux per RC (at $t = 0$)
$DI_0/CS_0 = (ABS/CS_0) - (TR_0/CS_0)$	Dissipated energy flux per CS (at $t = 0$)
Performance indexes	
$PI_{ABS} = (RC/ABS) \cdot [\varphi_{P0}/(1 - \varphi_{P0})] \cdot [\psi_0/(1 - \psi_0)]$	Performance index (PI) on absorption basis
$PI_{CS} = (RC/CS_0) \cdot [\varphi_{P0}/(1 - \varphi_{P0})] \cdot [\psi_0/(1 - \psi_0)]$	PI on cross section basis (at $t = 0$)

treatment (Fig. S1B). Thus, the shoot biomass cannot be used as an indicator to distinguish the low- and high-DBP accumulators.

3.2. Chlorophyll concentration and leaf ultrastructure

Total Chl concentrations in leaves of *Huaguan* presented no significant changes ($P > 0.05$) with increasing DBP levels in soil (Table 2). However, compared with the control, total Chl concentration in leaves of *Lvbao70* increased significantly ($P < 0.05$) under low DBP treatment, but decreased significantly ($P < 0.05$) under high DBP treatment. Furthermore, as shown in Table 2, the Chl a/Chl b ratio, which is a stress indicator, did not differ significantly ($P > 0.05$) between *Lvbao70* and *Huaguan* under both levels of DBP exposure.

TEM observation revealed that the leaves of both of the cultivars presented well-organised structures containing definite cell walls, chloroplasts, mitochondria, and clear nuclei in both CK (Fig. 1A and D) and low DBP treatments (Fig. 1B and E). The shuttle-like chloroplasts were of integrity, with tightly stacking lamellae of grana. There were few differences in chloroplast structures between the two cultivars, except that starch grains in the chloroplasts of *Lvbao70* were smaller. However, obvious changes in cell ultrastructures were observed in both cultivars under high DBP treatment. Especially, the chloroplasts and mitochondria swelled, and the amount of integrated chloroplasts decreased (Fig. 1C and F). Compared with *Huaguan*, *Lvbao70* suffered greater damage in chloroplast structures. For example, more thylakoids in chloroplasts of *Lvbao70* were grouped in irregular morphology and gradually disintegrated, and more starch grains disappeared and more osmiophilic plastoglobules accumulated in the chloroplasts (Fig. 1F). The results provided direct evidence that *Lvbao70* performed a lower tolerance to DBP toxicity than *Huaguan* did.

3.3. Leaf gas exchange

The leaf gas exchange parameters (including Pn, Gs, Ci, and E) of

Table 2
Mean (±SE, $n = 6–10$) net photosynthetic rate (Pn), intercellular CO_2 concentration (Ci), stomatal conductance (Gs), transpiration rate (E), total chlorophyll content (Chl a + b), and Chl a/b ratio in leaves of two Chinese flowering cabbage cultivars exposed to DBP treatments and control conditions.

DBP treatments (mg kg^{-1})	Cultivars	Pn (μmol m^{-2} s^{-1})	Ci (μmol mol^{-1})	Gs (mol m^{-2} s^{-1})	E (mmol m^{-2} s^{-1})	Toal chl content (mg g^{-1})	Chl a/b ratio
0 (control)	Lvbao70	11.18 ± 0.72a[a]	193 ± 11b	0.18 ± 0.02b	3.02 ± 0.16b	1.24 ± 0.16b	2.44 ± 0.16a
	Huaguan	10.87 ± 0.65a	186 ± 17b	0.19 ± 0.01b	3.87 ± 0.23a	1.18 ± 0.13b	2.58 ± 0.13a
10	Lvbao70	12.75 ± 1.12a	199 ± 14b	0.18 ± 0.01b	3.16 ± 0.22b	1.47 ± 0.14a	2.57 ± 0.20a
	Huaguan	11.74 ± 0.59a	202 ± 12b	0.24 ± 0.02a	4.24 ± 0.22a	1.31 ± 0.16 ab	2.62 ± 0.22a
100	Lvbao70	5.62 ± 0.34c	248 ± 16a	0.10 ± 0.01d	2.54 ± 0.14c	0.89 ± 0.08c	2.71 ± 0.17a
	Huaguan	8.79 ± 0.82b	196 ± 13b	0.13 ± 0.01c	3.19 ± 0.21b	1.14 ± 0.11b	2.74 ± 0.23a

[a] Means (±SE, $n = 6–10$) followed by the same letters within a column are not significantly different ($P > 0.05$).

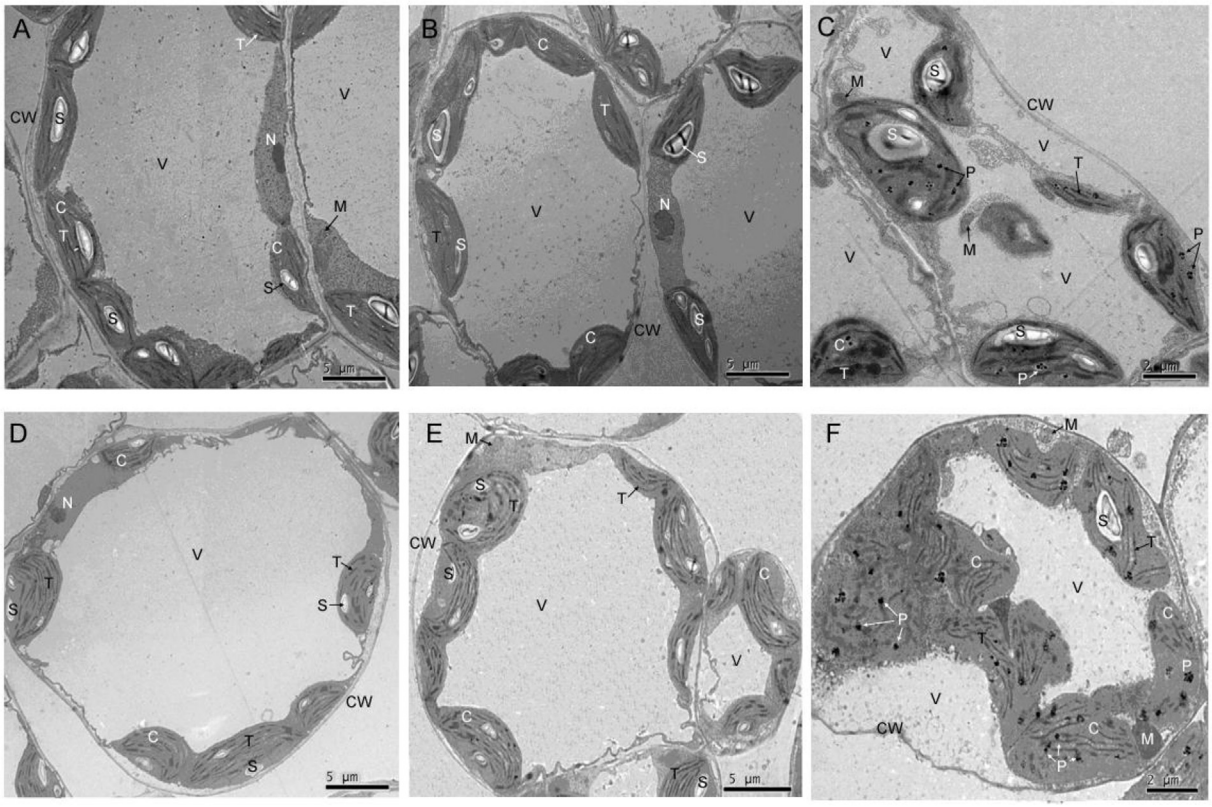

Fig. 1. Transmission electron microscopy of mesophyll cell of two Chinese flowering cabbage cultivars in different DBP treatments. (A–C) *Huaguan* treated with 0, 10, and 100 mg kg^{-1} DBP, respectively; (D–F) *Lvbao70* treated with 0, 10, and 100 mg kg^{-1} DBP, respectively. CW: cell wall; C: chloroplast; M: mitochondrion; N: nucleus; S: starch grain; T: thylakoid lamellae; V: vacuole; P: plastoglobuli.

both cultivars were comparable between low DBP treatment and the control, but the values of Pn and Gs of both cultivars decreased significantly under high DBP exposure. Moreover, Pn, Gs, and E values of *Lvbao70* decreased more sharply (49.73%, 44.44%, and 15.89%, respectively, compared with the control) than those of *Huaguan* (Table 2). These results indicated that CO_2 assimilation in leaves of *Lvbao70* was inhibited more seriously under high DBP exposure. Additionally, it should be noted that the E and Gs values of *Huaguan* were significantly higher than those of *Lvbao70* under the same DBP exposure (26–34% for E, and 33–36% for Gs under two levels of DBP exposure) (Table 2). The differences in E and Gs might play a role in DBP accumulation variation in the two cultivars.

3.4. Chlorophyll a fluorescence transient and related parameters

The leaves in both the control and DBP treatments showed typical polyphasic increases in Chl a fluorescence (Fig. 2A). The OJIP transients of both cultivars under low DBP treatment were similar to those of the control (except a slight increase at the P-step of *Lvbao70*) (Fig. 2B, presenting OJIP data as the kinetics of relative variable fluorescence at any time, $V_t = (F_t - F_0)/(F_m - F_0)$). However, under high DBP exposure, the OJIP transients of both cultivars showed an increase at the O-step and a decrease at the P-step (Fig. 2A), and an increase in the K-band (300 μs) was observed in the relative variable fluorescence (especially for *Lvbao70*) (Table 3). The values of fluorescence parameters derived from transient changes were analyzed in detail and the results were presented in Table 3 and Fig. 3.

No significant influences of low DBP exposure were observed on F_0, F_m, $F_{50\mu s}$, $F_{100\mu s}$, $F_{300\mu s}$, F_J, F_I, t_{Fm}, and *Area* in leaves of both cultivars compared with the control (except some increases in F_m, F_J, and F_I for *Lvbao70*) (Table 3). However, the values of F_0, $F_{50\mu s}$, $F_{100\mu s}$, $F_{300\mu s}$, and t_{Fm}, of both cultivars increased, while those of F_m, F_I, and *Area* decreased under high DBP exposure. Moreover, the values of F_0, $F_{50\mu s}$, $F_{100\mu s}$, $F_{300\mu s}$, t_{Fm}, and *Area* for *Lvbao70* were higher, but its F_m and F_I were lower than those of *Huaguan*. The fluorescence parameters can be derived in several ways, such as based on changes per CS_0 or changes per *RC*. Several parameters including *ABS* (absorbance), ET_0 (electron transport), TR_0 (trapping), and DI_0 (dissipation) per CS_0 were calculated from the OJIP curves (Table 1 and Fig. 3). Fig. 3A showed the behavior of 17 biophysical parameters of PSII. For each parameter, its value was normalized to the control value of *Huaguan*. Under two levels of DBP exposure, the data of *Lvbao70* and *Huaguan* could yield consistent estimates for most of the parameters. In general, slight

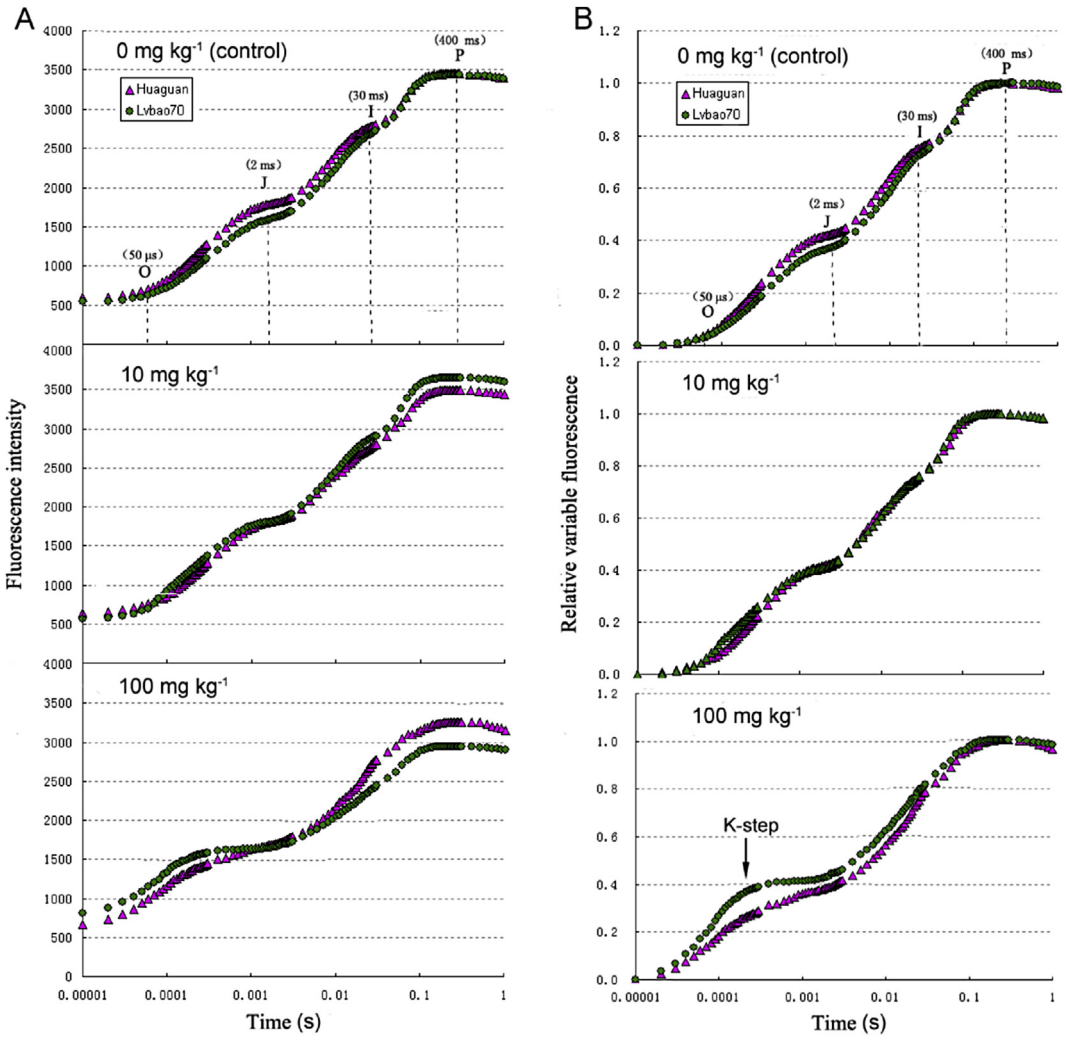

Fig. 2. Comparison of the OJIP chlorophyll a fluorescence transients (A) and relative variable fluorescence (B) between *Huaguan* and *Lvbao70* under the indicated concentrations of DBP. The graphs present mean transients of all measured samples ($n = 11$).

Table 3
Effects of DBP (mg kg^{-1}) reflected in data extracted from the recorded chlorophyll a fluorescence transient of two cultivars of *B. parachinensis*.

DBP	Cultivars	F_0	F_m	$F_{50\mu s}$	$F_{100\mu s}$	$F_{300\mu s}$	F_J	F_I	t_{Fm}	*Area*
0	Lvbao70	546 ± 27c[a]	3434 ± 59b	634 ± 45c	792 ± 45c	1160 ± 38c	1618 ± 45b	2747 ± 79b	289 ± 17c	63949 ± 2461a
	Huaguan	569 ± 22c	3452 ± 66b	654 ± 24c	823 ± 28c	1173 ± 46c	1870 ± 54a	2799 ± 54b	302 ± 14c	62254 ± 2194a
10	Lvbao70	566 ± 29c	3695 ± 84a	672 ± 30c	895 ± 37bc	1166 ± 34c	1824 ± 39a	2907 ± 82a	271 ± 23c	63017 ± 2156a
	Huaguan	587 ± 35c	3374 ± 73b	689 ± 32c	850 ± 38c	1207 ± 47c	1826 ± 42a	2801 ± 91 ab	290 ± 12c	63866 ± 1899a
100	Lvbao70	816 ± 57a	2957 ± 62d	1084 ± 36a	1342 ± 55a	1589 ± 57a	1611 ± 56b	2424 ± 63d	388 ± 20a	43482 ± 1563b
	Huaguan	684 ± 36b	3211 ± 56c	939 ± 41b	1167 ± 34b	1396 ± 59b	1578 ± 25b	2617 ± 68c	339 ± 18b	52086 ± 1714c

[a] Means ± SE ($n = 6–10$) followed by the same letters within a column are not significantly different ($P > 0.05$).

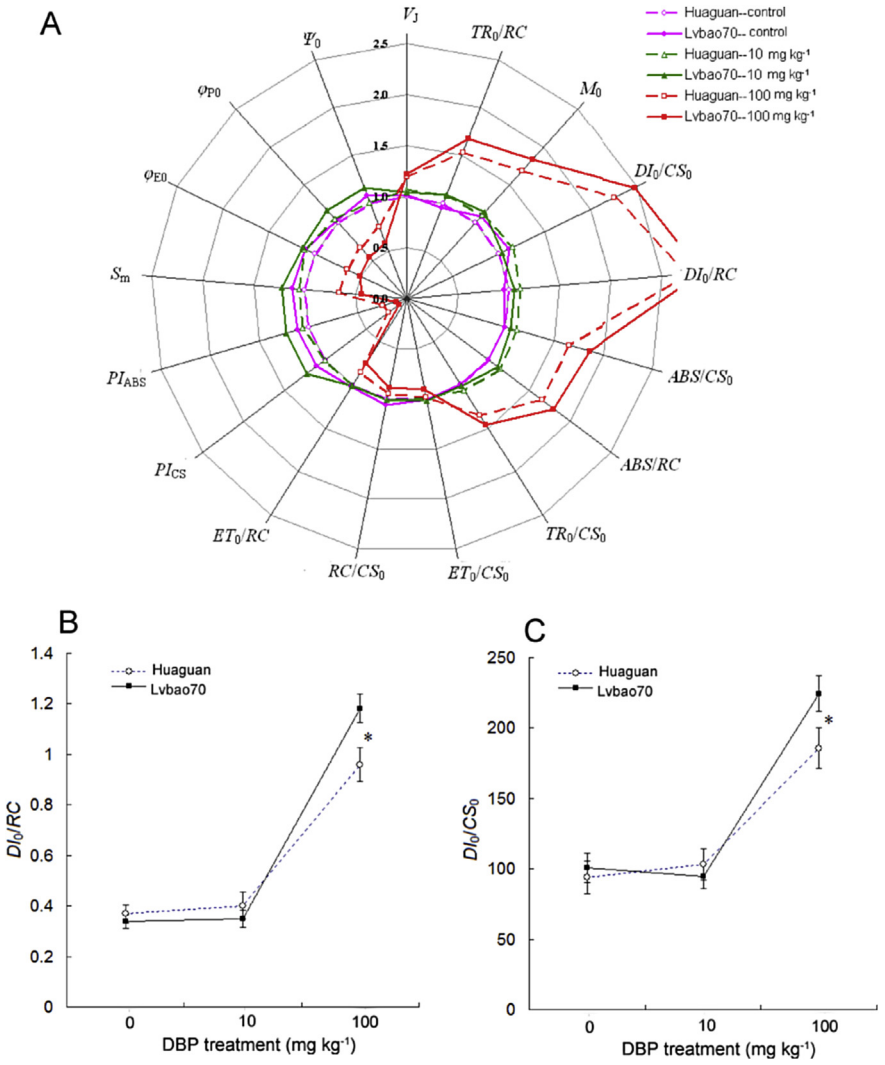

Fig. 3. (a) Spider plot (A) indicating selected OJIP parameters for *Huaguan* and *Lvbao70* of *B. parachinensis* in control and DBP treatments, all the values were normalized to the *Huaguan* control as 1. (b) B and C indicated the response of non-photochemical energy dissipation of two cultivars to DBP treatments. * indicated that the difference between two cultivars in the same treatment was significant ($P < 0.05$).

increases in TR_0/RC, M_0, DI_0/CS_0, DI_0/RC, ABS/CS_0, ABS/RC, TR_0/CS_0, ET_0/CS_0, RC/CS_0, ET_0/RC, PI_{CS}, PI_{ABS}, S_m, φ_{E0}, φ_{P0}, and Ψ_0 of both cultivars were observed under low DBP exposure, while significant increases in DI_0/RC, DI_0/CS_0, ABS/CS_0, ABS/RC, TR_0/RC, M_0 and TR_0/CS_0, and significant decreases in PI_{ABS}, PI_{cs}, S_m, ET_0/RC, φ_{E0}, φ_{P0}, and Ψ_0, were observed under high DBP exposure. Notably, there were significant differences ($P < 0.05$) in both DI_0/RC (Fig. 3B) and DI_0/CS_0 (Fig. 3C) between the two cultivars under high DBP exposure, which indicated that the two cultivars had different tolerance to photoinhibition.

3.5. Responses of antioxidases and MDA in plants

As shown in Fig. 4, the activities of SOD and GST in the shoots and roots of both cultivars increased significantly under DBP exposures. The activities of SOD and GST in the shoots and roots of *Lvbao70* were higher than or similar to those of *Huaguan* under low DBP exposure, but significantly lower under high DBP exposure. However, no significant difference in CAT activities was recorded between the two cultivars.

The responses of MDA to DBP treatments were approximately

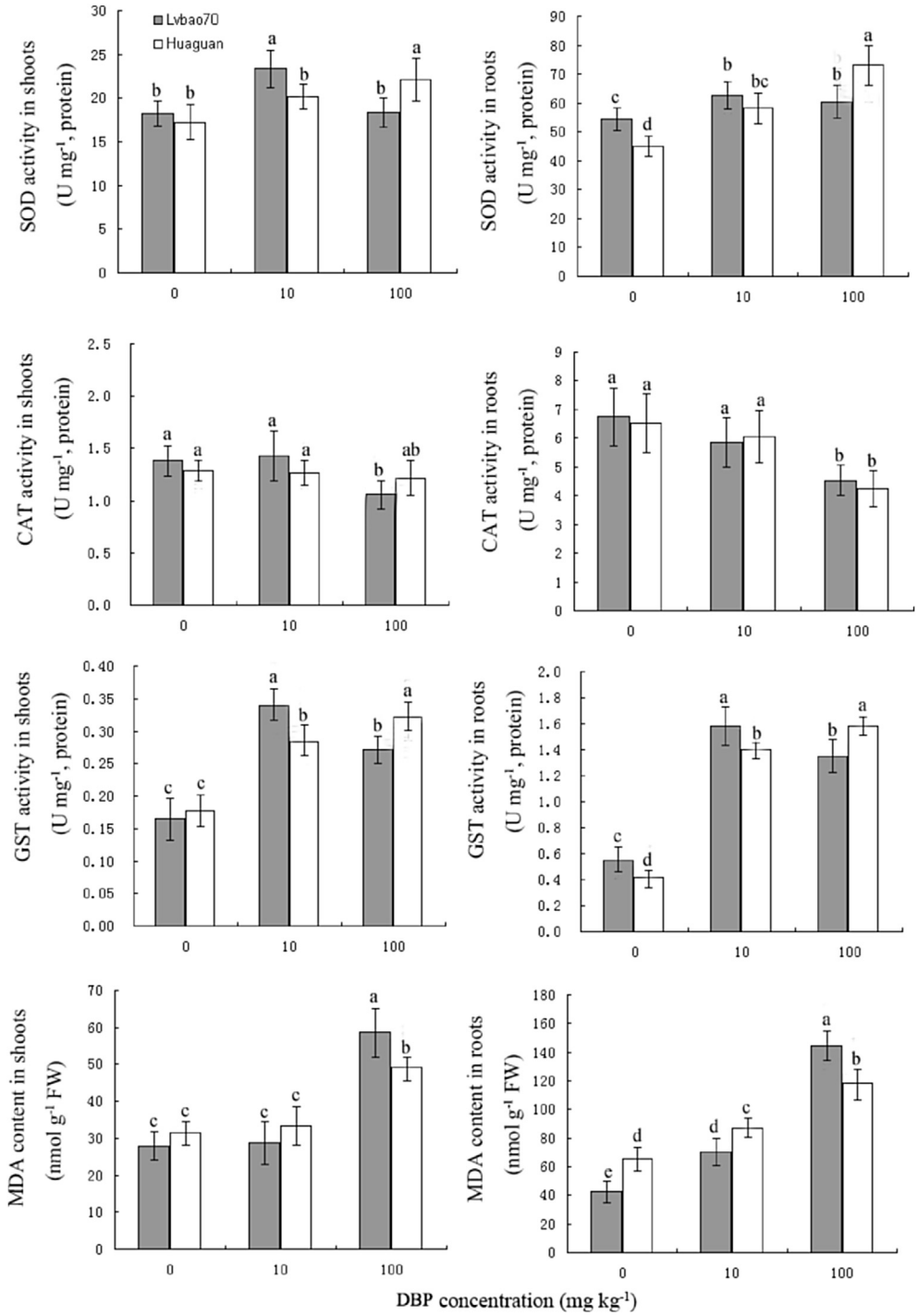

Fig. 4. Activities of superoxide dismutase (SOD), catalase (CAT), and glutathione S-transferase (GST), as well as malondialdehyde (MDA) content, in shoots and roots of two cultivars of *B. parachinensis*. The same letters indicate non-significant differences ($P > 0.05$).

dose-dependent, and the MDA content in both shoots and roots increased with increasing DBP concentration in soil, implying a certain lipid peroxidation damage of plant cells induced by DBP. The highest MDA content in the roots of *Lvbao70* was nearly 3.5-fold compared with the control. The MDA content in both shoots and roots of *Lvbao70* was lower than those in *Huaguan* under low DBP exposure, but significantly higher under high DBP exposure.

4. Discussion

Ultrastructural investigation showed that *Lvbao70* suffered greater damage in the structures of mesophyll cells than *Huaguan* did (Fig. 1C and F), which provide a direct evidence that *Lvbao70* is more sensitive to DBP toxicity. Especially, lots of starch grains disappeared and many chloroplasts exhibited remarkable disintegration, suggesting that DBP in *Lvbao70* induced more disturbances in

metabolic functions and lipid composition of membranes (Zhang et al., 2015a). Meanwhile, more plastoglobulis were observed in the chloroplasts of *Lvbao70*, which indicated that the function of the chloroplast in *Lvbao70* decreased to a greater extent because the pathways to form protein-containing cell structures were suppressed (Hoziner et al., 2009). In comparison, the cell structure of *Huaguan* displayed a larger increase in cell wall thickness and cytoplasmic vacuolization, suggesting a better cellular defense or detoxification mechanism against DBP exposure. It is well documented that a high tolerance of plants to contaminants coupled with an increased capacity of contaminant accumulation may attribute to an efficient detoxification mechanism in plant cells (Rascio and Navari-Izzo, 2011; Nehnevajova et al., 2012). Therefore, it was likely to cause toxic damages to the organelles of the low-tolerance *Lvbao70* when DBP levels in the mesophyll cells were high enough to result in phytotoxicity. However, the sensitive *Lvbao70* minimized DBP accumulation in mesophyll cells to protect its organelles from toxicity. As showed in Fig. S1A, the DBP concentrations of the roots in *Lvbao70* were significantly higher than those in *Huaguan*, which is consistent with our previous results that *Lvbao70* possesses a greater ability to prevent DBP from translocating from the roots to the shoots (Zhao et al., 2015). Especially, thinned cell wall and the irregular cytoplasmic vacuolization in mesophyll cells of *Lvbao70* (Fig. 1F) suggested a worse cellular defense or detoxification mechanism against DBP stress, which was not favorable for DBP accumulation in its cell walls or vacuoles (Zhang et al., 2015b). This inference was confirmed by the observation that *Lvbao70* had a lower proportion of DBP in the cell walls of the shoot than *Huaguan* did (Zhao et al., 2015). Overall, *Lvbao70* showed a lower tolerance to DBP toxicity than *Huaguan* did, which might account for its lower DBP accumulation to protect itself from toxicity.

As an important marker of internal plant metabolism, photosynthesis under any inhibition would adversely affect physiological activities during plant growth (Li et al., 2013). The gas exchange of many semivolatile organic compounds between plant leaves and air was considered to partly control the uptake and accumulation of these chemicals by plants (Tao and Hornbuckle, 2001). In this study, the high DBP exposure resulted in significant decreases in Pn, Gs, and E (Table 2), suggesting that a stomatal effect could be involved in the photosynthetic response of plants to DBP stress (Su et al., 2013). Higher Gs observed in *Huaguan* indicated less stomatal resistance, which was directly associated with the diffusion of organic pollutants through the stomata (Oguntimehin et al., 2008). It was such effect that might lead to enhanced uptake and accumulation of DBP by *Huaguan* through the stomata. In addition, the Ci of leaves increased significantly with the decrease in Gs and E, suggesting that the decrease of Pn in leaves of *Lvbao70* might be mainly attributable to non-stomatal limitation (Ahammed et al., 2012). Compared with *Lvbao70*, the unaffected Ci and a lower decrease of Gs and E in the leaves of *Huaguan* might lead to its higher Pn. The higher photosynthetic efficiency of *Huaguan* might correlate with its elevated DBP-tolerant mechanisms, which allowed *Huaguan* to accumulate more DBP. In addition, plant transpiration might play an important role in the uptake and translocation of organic contaminants (Gao and Collins, 2009; Dodgen et al., 2015). Some studies reported that high transpiration induced greater uptake of contaminants by plants than low transpiration did (Liao et al., 2006; Dodgen et al., 2015). In this study, the difference of DBP accumulation in the two cultivars could partly attribute to the difference in transpiration (Table 2). However, the quantitative contribution of transpiration to the uptake and accumulation of DBP by plants merits further investigation.

Chlorophyll is an important component that plays a role in energy production through photosynthesis. Compared with *Huaguan*, *Lvbao70* showed a significant decrease in the total chlorophyll content (Table 2), which might be due to its easier degradation or decreased synthesis when exposure to DBP (Váňová et al., 2009). Correspondingly, their ultrastructural observations also displayed obvious structural changes in chloroplasts, including modification in the quantity, size, and the organization of thylakoids (Fig. 1). Therefore, the reduction in Pn in *Lvbao70* was likely to be attributable to the reduction of leaf pigment and the damage of chloroplast (Su et al., 2013). Furthermore, our results clearly showed that DBP inhibited the photoactivation of PSII. The decreases in fluorescence intensity in both cultivars under high DBP exposure were pronounced within the JI and IP phases (Fig. 2A). The intensity during the OJ phase associated with accumulation of Q_A^- shifted to a lesser degree. The decrease in the IP phase detected in this study could be associated with blocking of the electron transfer from Q_A to Q_B, likely due to the increase in the fraction of Q_B-nonreducing centers (Tomar and Jajoo, 2013). Meanwhile, the decreased extents of F_j, F_i, and F_m were higher in *Lvbao70* than in *Huaguan* (Table 3), suggesting that electron transport at the donor side of PS II was inhibited more seriously in the former (Aksmann and Tukaj, 2008). Besides, the increased F_0 for *Lvbao70* exposed to DBP (Fig. 2A and Table 3) might be due to the increased number of inactive RCs (where electrons cannot be transferred from reduced Q_A) and the low energy transfer from the light-harvesting complex II to the PSII reaction center, and thus higher fluorescence from light-harvesting complex II (Tomar and Jajoo, 2013). From the kinetics of the relative variable fluorescence, a positive K-step appeared at 300 μs in the OJIP transients of *Lvbao70* under high DBP exposure (Fig. 2B). This suggested that the oxygen-evolving complex in the leaves of *Lvbao70* was more easily damaged, which inhibited the electron donation from water to the secondary electron donor of PSII (Hakala et al., 2005). Similar results were also observed in *Desmodesmus subspicatus* exposed to anthracene (Baścik-Remisiewicz et al., 2011).

Furthermore, fluorescence parameters suggested that the inhibition of photosynthetic activity of both cultivars exposed to high levels of DBP resulted from the impairment of primary photochemical processes (Fig. 3A). Most of the parameters indicated that PSII was more photo-inhibited in *Lvbao70* than in *Huaguan*. Especifically, DBP decreased the total electron acceptor capacity in the leaves of *Lvbao70* more strongly than that in *Huaguan*, as indicated by the decreased S_m (Fig. 3A), which could measure the pool of electron transporters between PSII and the acceptor side of PSI (Pinior et al., 2005). The leaves exposed to DBP also presented a lower ET_0/CS_0 than those in the control, but an increased TR_0/CS_0 (Fig. 3A), indicating that DBP affected the activity of electron transport chain, especially in *Lvbao70* (Jiang et al., 2008). As demonstrated by Strasser et al. (2000), the decrease in the performance index (PI) might result from a disruption of energy absorption, trapping, or transfer beyond Q_A quinone. In this study, the decreases in both PI_{ABS} and PI_{CS} in both cultivars exposed to DBP were due to low quantum efficiency of electron trapping and transport (ψ_0, φ_{P0}, φ_{E0}) (Fig. 3A). The efficiency by which a trapped electron can move further ahead of Q_A^- is equal to $1 - V_J$ (i.e. ψ_0) (Tomar and Jajoo, 2013). Moreover, a significant decrease was observed in the value of ψ_0 in both cultivars under high DBP exposure, especially in *Lvbao70* (Fig. 3A), suggesting that Q_A^- electron transport at the acceptor side of PSII was blocked. Besides, the reduction in F_v/F_m (i.e. φ_{P0}), which is a good indicator of photoinhibitory effects on PSII, was caused by both a decrease in F_m and an increase in F_0 (Table 3) (Maxwell and Johnson, 2000).

In addition, the decreased RC/CS_0 (Fig. 3A), implied that elevated F_0 might be induced by the inactivation of some of the PSII RCs (Yamane et al., 1997) or be related to the accumulation of reduced Q_A caused by the fractional reduction of Q_A to Q_A^- (Bukhov et al.,

1990), as indicated by the increase in M_0 (Fig. 3A). However, when considering the specific energy fluxes for energy absorption (*ABS*/*RC*) and trapping (TR_0/*RC*), a significant increase in all fluxes occurred (Fig. 3A), implying that a greater antenna size and photosynthetic activity of single RC in plants exposed to high DBP than those in the control and those to low DBP treatment. Meanwhile, under high DBP exposure, the increase in *ABS*/*RC* and TR_0/*RC* of *Lvbao70* was higher than that of *Huaguan*. Nevertheless, ET_0/*RC* did not decrease in either cultivar exposed to DBP. Thus, when energy absorption was much higher than energy utilization, the PSII over-excitation must be quenched non-photochemically to avoid damage to the photosystem (Tomar and Jajoo, 2013). As expected, the indicators of non-photochemical energy dissipation, DI_0/*RC* and DI_0/CS_0, increased significantly in both cultivars in high DBP treatment (Fig. 3A). Especially, such an increase in *Lvbao70* was significantly greater ($P < 0.05$) than that in *Huaguan*. Compared with the *Huaguan*, *Lvbao70* utilized only a smaller fraction of the absorbed light energy in photosynthetic electron transport, as indicated by more decreases in ET_0/*RC*, ψ_0, φ_{P0}, and φ_{E0} (Fig. 3A), suggesting more excess excitation energy existed in *Lvbao70*, which could further lead to the production of ROS, and caused damage to photosynthetic apparatus (Song et al., 2006). These results revealed that PSII in *Lvbao70* was photo-inhibited more seriously than that in *Huaguan* (Yang et al., 2012). Therefore, the lower DBP-tolerance of *Lvbao70* could be associated with its poor photosynthesis performance, which may function as a mechanism for accumulation of a lower amount of DBP.

To combat ROS induced by DBP, plants are endowed with an efficient enzymatic antioxidant system including CAT, SOD, and GST (Zhang et al., 2015a). Under low DBP exposure, the higher activities of SOD and GST were recorded in both the shoots and the roots of *Lvbao70* compared to *Huaguan* (Fig. 4), suggesting that SOD and GST might play critical roles in the hormetic response of *Lvbao70* to DBP. Accordingly, a "stimulative effect" occurred on the shoot biomass of *Lvbao70* (Fig. S1B). The result suggested that the organic chemical-induced ROS production could trigger antioxidant defenses that induced hormetic responses under certain conditions (Hashmi et al., 2014). However, under high DBP exposure, the activities of SOD and GST in the both shoots and the roots of *Lvbao70* were significantly lower than those of *Huaguan* (Fig. 4), indicative of a loss of protective capacity in *Lvbao70* against cellular superoxide toxicity under increased DBP concentration. This may result from the breakdown of the antioxidant system when DBP level was high enough to cause phytotoxicity (He et al., 2013). These results are consistent with our observation that *Lvbao70* is more sensitive to DBP toxicity than *Huaguan* due to lack of a more powerful antioxidant capability. Additionally, it should be noted that among the antioxidant enzymes, the CAT activities of both cultivars decreased under high DBP exposure and were not significantly different (Fig. 4). The decreases of CAT activities might be related to the fact that the CAT was more sensitive to DBP toxicity than other antioxidant enzymes, and it is likely that there is a chloroplast-mediated CAT inactivation caused by oxidative damage (Yang et al., 2012). Besides, no significant difference was observed for MDA content in the shoots of *Lvbao70* between in the control and low-DBP treatment (Fig. 4), which confirmed the beneficial effects on the photosynthetic system under low DBP exposure, as mentioned above. However, the significant increases in MDA content were observed in both the shoots and the roots of the two cultivars under high DBP exposure, especially in *Lvbao70* (Fig. 4), suggestive of greater damage to *Lvbao70* than *Huaguan* as a result of lipid peroxidation. Overall, these results indicated that a weaker antioxidant capacity of *Lvbao70* might be associated with its lower DBP accumulation.

5. Conclusions

Our data support the hypothesis that the physiological responses of Chinese flowering cabbage to DBP stress differ significantly between the low- and high-DBP cultivars. Compared with *Huaguan*, *Lvbao70* suffered more adverse effects under high DBP exposure which resulted in greater damage to the photosynthetic system. The result showed that *Lvbao70* was more sensitive to DBP toxicity than *Huaguan* was, which might account for its decreased DBP accumulation to protect against toxicity. However, it requires further study on the functional mechanism that underlies physiological differences in DBP-accumulation between low and high accumulators.

Acknowledgments

This work was funded by the National Natural Science Foundation of China (41173101, 41301337, 41273113, and 41573093), the NSFC-Guangdong Joint Fund (U1501233), the Fundamental Research Funds for the Central Universities (21612103, 21613403), the project on the Integration of Industry, Education and Research of Guangdong Province (2013B0906001) and the High-Level Talents Program of Guangdong Higher Education Institutions, granted to C.-H. Mo.

Appendix A. Supplementary data

Supplementary data related to this article can be found at http://dx.doi.org/10.1016/j.envpol.2015.11.009.

References

Ahammed, G.J., Yuan, H.L., Ogweno, J.O., Zhou, Y.H., Xia, X.J., Mao, W.H., Shi, K., Yu, J.Q., 2012. Brassinosteroid alleviates phenanthrene and pyrene phytotoxicity by increasing detoxification activity and photosynthesis in tomato. Chemosphere 86, 546–555.

Aksmann, A., Tukaj, Z., 2008. Intact anthracene inhibits photosynthesis in algal cells: a fluorescence induction study on *Chlamydomonas reinhardtii* cw92 strain. Chemosphere 74, 26–32.

Baścik-Remisiewicz, A., Aksmann, A., Żak, A., Kowalska, M., Tukaj, Z., 2011. Toxicity of cadmium, anthracene, and their mixture to *Desmodesmus subspicatus* estimated by algal growth-inhibition ISO standard test. Arch. Environ. Contamin. Tox. 60, 610–617.

Bukhov, N.G., Sabat, S.C., Mohanty, P., 1990. Analysis of chlorophyll a fluoresence changes in weak light in heat treated *Amaranthus chloroplasts*. Photosynth. Res. 23, 81–87.

Cai, Q.Y., Mo, C.H., Wu, Q.T., Katsoyiannis, A., Zeng, Q.Y., 2008. The status of soil contamination by semivolatile organic chemicals (SVOCs) in China: a review. Sci. Total Environ. 389, 209–224.

Cai, Q.Y., Mo, C.H., Wu, Q.T., Zeng, Q.Y., Katsoyiannis, A., 2007. Quantitative determination of organic priority pollutants in the composts of sewage sludge with rice straw by gas chromatography coupled with mass spectrometry. J. Chromatogr. A 1143, 207–214.

Dodgen, L.K., Ueda, A., Wu, X.Q., Parker, D.R., Gan, J., 2015. Effect of transpiration on plant accumulation and translocation of PPCP/EDCs. Environ. Pollut. 198, 144–153.

Gao, Y., Collins, C.D., 2009. Uptake pathways of polycyclic aromatic hydrocarbons in white clover. Environ. Sci. Technol. 43, 6190–6195.

Gill, S.S., Tuteja, N., 2010. Reactive oxygen species and antioxidant machinery in abiotic stress tolerance in crop plants. Plant Physiol. Biochem. 48, 909–930.

Hakala, M., Tuominen, I., Keränen, M., Tyystjärvi, T., Tyystjärvi, E., 2005. Evidence for the role of the oxygen -evolving manganese complex in photoinhibition of photosystem II. BBA-Bioenergetics 1706, 68–80.

Hashmi, M.Z., Shen, H., Zhu, S., Yu, C.N., Shen, C.F., 2014. Growth, bioluminescence and shoal behavior hormetic responses to inorganic and/or organic chemicals: a review. Environ. Int. 64, 28–39.

He, Y., Dai, S., Dufresne, C.P., Zhu, N., Pang, Q.Y., Chen, S.X., 2013. Integrated proteomics and metabolomics of arabidopsis acclimation to gene-dosage dependent perturbation of isopropylmalate dehydrogenases. Plos One 8, e57118.

Holzinger, A., Roleda, M.Y., Lütz, C., 2009. The vegetative arctic freshwater green alga Zygnema is insensitive to experimental UV exposure. Micron 40, 831–838.

Hu, H.Q., Wang, L.H., Wang, Q.Q., Jiao, L.Y., Hua, W.Q., Zhou, Q., 2014. Photosynthesis, chlorophyll fluorescence characteristics, and chlorophyll content of soybean seedlings under combined stress of bisphenol A and cadmium. Environ. Toxicol. Chem. 33, 2455–2462.

Jiang, H.X., Chen, L.S., Zheng, J.G., Han, S., Tang, N., Smith, B.R., 2008. Aluminum-induced effects on photosystem II photochemistry in citrus leaves assessed by the chlorophyll a fluorescence transient. Tree Physiol. 28, 1863–1871.
Kumar, S., Asif, M.H., Chakrabarty, D., Tripathi, R.D., Dybey, R.S., Trivedi, P.K., 2013. Expression of a rice Lambda class of glutathione S-transferase, OsGSTL2, in *Arabidopsis* provides tolerance to heavy metal and other abiotic stresses. J. Hazard. Mater. 248, 228–237.
Li, Q.S., Lu, Y.L., Shi, Y.J., Wang, T.Y., Ni, K., Xu, L., Liu, S.J., Wang, L., Xiong, Q.L., Giesy, J.P., 2013. Combined effects of cadmium and fluoranthene on germination, growth and photosynthesis of soybean seedlings. J. Environ. Sci. 25, 1936–1946.
Liao, C.S., Yen, J.H., Wang, Y.S., 2009. Growth inhibition in Chinese cabbage (*Brassica rapa* var. chinensis) growth exposed to di-*n*-butyl phthalate. J. Hazard. Mater. 163, 625–631.
Liao, Y.C., Chang Chien, S.W., Wang, M.C., Shen, Y., Hung, P.L., Biswanath, D., 2006. Effect of transpiration on Pb uptake by lettuce and on water soluble low molecular weight organic acids in rhizosphere. Chemosphere 2, 343–351.
Liu, W., Zhang, C., Liu, S., 2014. Effects of phthalate ester treatment on seed germination and antioxidant enzyme activities of *Phaseolus radiatus* L. B. Environ. Contam. Tox. 92, 621–624.
Ma, T.T., Christie, P., Teng, Y., Luo, Y.M., 2013. Rape (*Brassica chinensis* L.) seed germination, seedling growth, and physiology in soil polluted with di-n-butyl phthalate and bis (2-ethylhexyl) phthalate. Environ. Sci. Pollut. R. 20, 5289–5298.
Ma, T.T., Christie, P., Luo, Y.M., Teng, Y., 2014. Physiological and antioxidant responses of germinating mung bean seedlings to phthalate esters in soil. Pedosphere 24, 107–115.
Maxwell, K., Johnson, G.N., 2000. Chlorophyll fluorescence-a practical guide. J. Exp. Bot. 51, 659–668.
Mo, C.H., Cai, Q.Y., Tang, S., 2009. Polycyclic aromatic hydrocarbons and phthalic acid esters in vegetables from nine farms of the Pearl River Delta, South China. Arch. Environ. Contam. Toxicol. 56, 181–189.
Mostofa, M.G., Hossain, M.A., Fujita, M., Tran, L.S., 2015. Physiological and biochemical mechanisms associated with trehalose-induced copper-stress tolerance in rice. Sci. Rep. 5, 11433.
Nehnevajova, E., Lyubenova, L., Herzig, R., Schröderb, P., Schwitzguébeld, J., Schmüllinga, T., 2012. Metal accumulation and response of antioxidant enzymes in seedlings and adult sunflower mutants with improved metal removal traits on a metal-contaminated soil. Environ. Exp. Bot. 76, 39–48.
Niu, L., Xu, Y., Xu, C., Yun, L., Liu, W., 2014. Status of phthalate esters contamination in agricultural soils across China and associated health risks. Environ. Pollut. 195, 16–23.
Oguntimehin, I., Nakatani, N., Sakugawa, H., 2008. Phytotoxicities of fluoranthene and phenanthrene deposited on needle surfaces of the evergreen conifer, Japanese red pine (*Pinus densiflora* Sieb. et Zucc.). Environ. Pollut. 154, 264–271.
Pietrini, F., Iori, V., Bianconi, D., Bianconi, D., Mughini, G., Massacci, A., Zacchini, M., 2015. Assessment of physiological and biochemical responses, metal tolerance and accumulation in two eucalypt hybrid clones for phytoremediation of cadmium-contaminated waters. J. Environ. Manage. 162, 221–231.
Pinior, A., Grunewaldt-Stöcker, G., von Alten, H., Strasser, R.J., 2005. Mycorrhizal impact on drought stress tolerance of rose plants probed by chlorophyll a fluorescence, proline content and visual scoring. Mycorrhiza 15, 596–605.
Rascio, N., Navari-Izzo, F., 2011. Heavy metal hyperaccumulating plants: how and why do they do it? And what makes them so interesting? Plant Sci. 180, 169–181.
Schecter, A., Lorber, M., Guo, Y., Wu, Q., Yun, S.H., Kannan, K., Hommel, M., Imran, N., Hynan, L.S., Cheng, D.L., Colacino, J.A., Birnbaum, L.S., 2013. Phthalate concentrations and dietary exposure from food purchased in New York State. Environ. Health. Perspec. 121, 473–479.
Strasser, R.J., Srivastava, A., Tsimilli-Michael, M., 2000. The fluorescence transient as a tool to characterize and screen photosynthetic samples. In: Yunus, M., Pathre, U., Mohanty, P. (Eds.), Probing Photosynthesis Mechanisms Regulation and Adaptation. Taylor and Francis, London–New York.
Song, Y.G., Liu, B., Wang, L.F., Li, M.H., Liu, Y., 2006. Damage to the oxygen-evolving complex by superoxide anion, hydrogen peroxide, and hydroxyl radical in photoinhibition of photosystem II. Photosynth Res. 90, 67–78.
Su, Y., Wang, X., Liu, C., Shi, G.R., 2013. Variation in cadmium accumulation and translocation among peanut cultivars as affected by iron deficiency. Plant Soil 363, 201–213.
Tao, Z., Hornbuckle, K.C., 2001. Uptake of polycyclic aromatic hydrocarbons (PAHs) by broad leaves: analysis of kinetic limitations. Water Air Soil Pollut. Focus 1, 275–283.
Tomar, S.R., Jajoo, A., 2013. Alteration in PS II heterogeneity under the influence of polycyclic aromatic hydrocarbon (fluoranthene) in wheat leaves (*Triticum aestivum*). Plant Sci. 209, 58–63.
Tsimilli-Michael, M., Strasser, R.J., 2008. In vivo assessment of stress impact on plant's vitality: applications in detecting and evaluating the beneficial role of mycorrhization on host plants. In: Varma, A. (Ed.), Mycorrhiza. Springer, Berlin Heidelberg, pp. 679–703.
Váňová, L., Kummerová, M., Klemš, M., Štěpán, Z., 2009. Fluoranthene influences endogenous abscisic acid level and primary photosynthetic processes in pea (*Pisum sativum* L.) plants in vitro. Plant Growth Regul. 57, 39–47.
Wang, J., Luo, Y., Teng, Y., Ma, W., Christie, P., Li, Z., 2013. Soil contamination by phthalate esters in Chinese intensive vegetable production systems with different modes of use of plastic film. Environ. Pollut. 180, 265–273.
Wang, J.L., Yuan, J.G., Yang, Z.Y., Huang, B.F., Zhou, Y.H., Xin, J.L., Gong, Y.L., Yu, H., 2009. Variation in cadmium accumulation among 30 cultivars and cadmium subcellular distribution in 2 selected cultivars of water spinach (*Ipomoea aquatica* Forsk.). J. Agr. Food Chem. 57, 8942–8949.
Yamane, Y., Kashino, Y., Koike, H., Satoh, K., 1997. Increases in the fluorescence Fo level and reversible inhibition of photosystem II reaction center by high-temperature treatments in higher plants. Photosynth. Res. 52, 57–64.
Yang, G.H., Yang, L.T., Jiang, H.X., Li, Y., Wang, P., Chen, L.S., 2012. Physiological impacts of magnesium-deficiency in citrus seedlings: photosynthesis, antioxidant system and carbohydrates. Trees 26, 1237–1250.
Yin, R., Lin, X.G., Wang, S.G., Zhang, H.Y., 2003. Effect of DBP/DEHP in vegetable planted soil on the quality of capsicum fruit. Chemosphere 50, 801–805.
Zhang, Y., Du, N., Wang, L., Zhang, H., Zhao, J., Sun, J., Wang, P., 2015a. Physical and chemical indices of cucumber seedling leaves under dibutyl phthalate stress. Environ. Sci. Pollut. R. 22, 3477–3488.
Zhang, Y., Tao, Y., Zhang, H., Wang, L., Sun, G.Q., Erinle, K.O., Feng, C.C., Song, Q.X., Li, M., 2015b. Effect of di-*n*-butyl phthalate on root physiology and rhizosphere microbial community of cucumber seedlings. J. Hazard. Mater. 289, 9–17.
Zhao, H.M., Du, H., Xiang, L., Chen, Y.L., Lu, L.A., Li, Y.W., Li, H., Cai, Q.Y., Mo, C.H., 2015. Variations in phthalate ester (PAE) accumulation and their formation mechanism in Chinese flowering cabbage (*Brassica parachinensis* L.) cultivars grown on PAE-contaminated soils. Environ. Pollut. 206, 95–103.